

# Characterization of Pure Nickel Coatings Fabricated under Pulse Current Conditions

M. Sajjadnejad, H. Omidvar, M. Javanbakht, A. Mozafari

**Abstract**—Pure nickel coatings have been successfully electrodeposited on copper substrates by the pulse plating technique. The influence of current density, duty cycle and pulse frequency on the surface morphology, crystal orientation, and microhardness was determined. It was found that the crystallite size of the deposit increases with increasing current density and duty cycle. The crystal orientation progressively changed from a random texture at 1 A/dm<sup>2</sup> to (200) texture at 10 A/dm<sup>2</sup>. Increasing pulse frequency resulted in increased texture coefficient and peak intensity of (111) reflection. An increase in duty cycle resulted in considerable increase in texture coefficient and peak intensity of (311) reflection. Coatings obtained at high current densities and duty cycle present a mixed morphology of small and large grains. Maximum microhardness of 193 Hv was achieved at 4 A/dm<sup>2</sup>, 10 Hz and duty cycle of 50%. Nickel coatings with (200) texture are ductile while (111) texture improves the microhardness of the coatings.

**Keywords**—Current density, Duty cycle, Microstructure, Nickel, Pulse frequency.

## I. INTRODUCTION

ELECTRODEPOSITION of nickel is widely used for both decorative and engineering purposes. Several additives are used to control the microstructure and morphology of the nickel electrodeposits and the current distribution. For those who partake in the nickel plating industry it would be a great simplification if the application of bath additives could be reduced or totally avoided [1]. Pulse electrodeposition method has been considered by many researchers as a promising alternative and several research works have been carried out over the past decade. While pulse plating cannot in fact replace the additives, it presents numerous interesting aspects. Pulse electroplating technique can be employed to improve the current distribution at the cathode surface and to modify the general mass transport conditions [2]. Besides, it can be used to control the microstructure of deposits, for example, nanocrystalline and multilayer coatings are actively reported [3], [4]. Moreover, pulse electroplating has been applied to

control the composition of electrodeposited alloys by changing the bath parameters [5].

In pulse electrodeposition method the duty cycle ( $\gamma$ ) is the ratio of time an individual pulse is ON compared to the total pulse time.  $\gamma$  can be calculated as [6]:

$$\text{Duty cycle } (\gamma) = \frac{T_{ON}}{T_{ON}+T_{OFF}} = T_{ON}f \quad (1)$$

where  $T_{ON}$  is ON-time,  $T_{OFF}$  is OFF-time and  $f$  is the pulse frequency. The pulse frequency is the number of times the current is switched on in a second and can be calculated as [6]:

$$f = \frac{1}{T_{on}+T_{off}} = \frac{1}{T} \quad (2)$$

where  $T$  is the total cycle time. The performance of pure nickel coatings depends on their microstructure (i.e., grain size, morphology and preferred crystallographic orientation) which is determined by the electroplating conditions and chemical composition of the plating bath. However, our knowledge of the evolution of nickel microstructure and morphology under pulse current conditions is limited. In the present paper, we investigate the effects of pulse plating parameters (current density, duty cycle and pulse frequency) on the microstructure and morphology of the nickel coatings.

## II. EXPERIMENTAL

Pulse electroplating conditions and bath composition are presented in TABLE I. NiSO<sub>4</sub> is the main source of Ni<sup>2+</sup> ions. The use of nickel sulfate is advantageous because it is readily soluble (650g/l at 20°C), cheap, commercially available and is one of the best sources of uncomplexed Ni<sup>2+</sup> ions. In nickel electroplating baths the activity of Ni<sup>2+</sup> ions is determined by the nickel salts content of the bath, the degree of dissociation and concentration of others components of the bath.

TABLE I  
ELECTROPLATING PARAMETERS AND CHEMICAL COMPOSITION OF THE BATH

Variable	Range
NiSO <sub>4</sub> .6H <sub>2</sub> O	300 (g/l)
H <sub>3</sub> BO <sub>3</sub>	40 (g/l)
NiCl <sub>2</sub> .6H <sub>2</sub> O	40 (g/l)
Peak current density	1, 4, 7, 10 (A/dm <sup>2</sup> )
Pulse frequency	1, 10, 50, 100 (Hz)
Duty cycle	10, 25, 50, 75 (%)
pH	4
Stirring rate	250 (rpm)

M. Sajjadnejad is with department of Mining and Metallurgical Engineering, Amirkabir University of Technology (Tehran Polytechnic), Tehran, Iran (corresponding author to provide phone: +989378730497; e-mail: m.sajjadnejad@yahoo.com).

H. Omidvar is with department of Mining and Metallurgical Engineering, Amirkabir University of Technology (Tehran Polytechnic), Tehran, Iran (e-mail: club.engineers@yahoo.com).

M. Javanbakht is with department of chemistry, Amirkabir University of Technology (Tehran Polytechnic), Tehran, Iran (e-mail: mohammadsajjadnejad@gmail.com).

A. Mozafari is with department of Materials Science and Engineering, Sharif university of Technology, Tehran, Iran (e-mail: alimozaffary\_mz@yahoo.com).

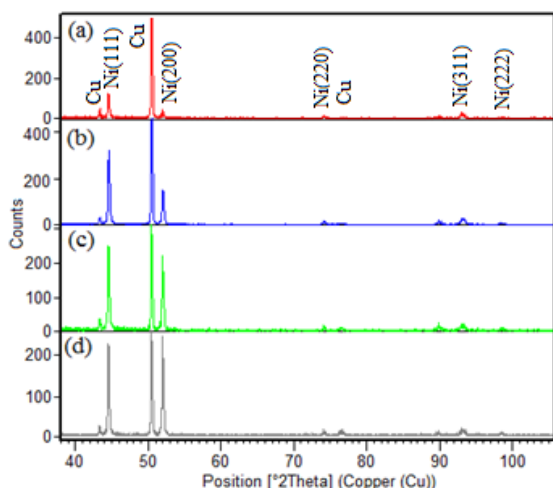


Fig. 1 XRD patterns of Ni electrodeposits obtained at (a)  $i_p = 1 \text{ A/dm}^2$  (b)  $i_p = 4 \text{ A/dm}^2$  (c)  $i_p = 7 \text{ A/dm}^2$  (d)  $i_p = 10 \text{ A/dm}^2$ :  
For all of these coatings  $\gamma = 50\%$  and  $f = 1 \text{ Hz}$

The addition of chloride salt has two major influences: it enhances anode corrosion and diffusion coefficient of  $\text{Ni}^{2+}$  ions thus allowing a higher limiting current density. Boric acid ( $\text{H}_3\text{BO}_3$ ) is added as a buffering agent to the Watts bath to maintain the pH of the solution at a fixed value [7].

Copper sheets (20 mm×10 mm×1 mm) were used as a substrate, and high purity electrolytic Ni plates (70 mm×20 mm×1 mm) were chosen as the soluble anode. Anodes surface area was 7 times greater than that of the copper cathode to make sure that anode polarization is avoided. This is particularly important at high current densities. The copper sheets were first polished and chemically degreased. Copper sheets were then acid cleaned and activated (HCl 15%), and finally washed with distilled water.

Scanning electron microscope (SEM, Cambridge S360) was employed to study the surface morphologies of the nickel electrodeposits. A Philips XPert-pro diffractometer was applied to investigate the microstructure of the Ni electrodeposits. The microhardness of the nickel electrodeposits was measured using the Leitzwetzlar Microhardness tester, applying a load of 10g.

### III. RESULTS AND DISCUSSION

#### A. X-ray Diffraction Spectrums

In order to achieve a better understanding of the effects of pulse plating parameters on the microstructure of Ni electrodeposits obtained from a Watts bath, X-ray diffraction analysis was conducted on the coatings plated under different plating conditions. At peak current density ( $i_p$ ) of  $1 \text{ A/dm}^2$  (111) crystal plane presented the highest peak intensity. However, at the peak current density of  $10 \text{ A/dm}^2$ , peak intensity of (200) was higher than peak intensity of (111). Increasing duty cycle lead to increased peak intensity of (111) crystal plane.

When  $\gamma = 10\%$ , the relative intensity of (111) was 100%, and the relative intensity of (200) was 87%; when  $\gamma = 25\%$ , relative

intensity of (111) was 100%, relative intensity of (200) was 47%, %; when  $\gamma = 50\%$ , relative intensity of (111) was 100%, relative intensity of (200) was 44%,%; when  $\gamma = 75\%$ , relative intensity of (111) was 100%, relative intensity of (200) was 21%.

The effect of pulse frequency on the microstructure of the nickel coatings was not significant. When  $f = 1 \text{ Hz}$  relative intensity of (111) was 100%, relative intensity of (200) was 21%; When  $f = 10 \text{ Hz}$  relative intensity of (111) was 100%, relative intensity of (200) was 44%; When  $f = 50 \text{ Hz}$  relative intensity of (111) was 100%, relative intensity of (200) was 42%; When  $f = 100 \text{ Hz}$  relative intensity of (111) was 100%, relative intensity of (200) was 28%. Hence, the maximum relative peak intensity of (200) occurs at  $f = 10 \text{ Hz}$ .

According to [8] variations in nickel microstructure under different plating conditions may be ascribed to:

1. The depletion of  $\text{Ni}^{2+}$  cations at the cathode surface; which is very important at high current densities and duty cycles and low pulse frequencies.
2. The thickness of the pulsating diffusion layer. In pulse current electrodeposition diffusion layer consists of a stationary layer and a pulsating layer [9].
3. The overpotential which mainly depends on current density [10].
4. Hydrogen adsorption/ evolution. Adsorption of  $\text{H}^+$  ions leads to electrocrystallization on (110) crystal plane [11].
5. Adsorption of insoluble ions such as  $\text{Ni}(\text{OH})_2$ .

#### B. Texture Coefficients

Almost in all of the industrial applications, in order to successfully satisfy the material requirements, a particular crystallographic is essential. It has been reported that the texture of the electrodeposited coatings is controlled by the electrodeposition parameters such as current density, stirring rate, pulse frequency, composition of the bath, duty cycle and so on [12]. For a more detailed investigation of the texture, texture coefficients (TC) of the main crystal planes of nickel deposits were determined. Texture coefficients present the preferred crystal orientation. TC values greater than 1 reveal a preferred growth. In order to study the preferred orientation of nickel coatings, the TC values were calculated as:

$$TC(hkl) = \frac{I(hkl)}{I_0(hkl)} \quad (3)$$

$$I_0(hkl) = \frac{1}{n} \sum I_0(hkl)$$

where  $I(hkl)$  is the measured intensity and  $I_0(hkl)$  is standard intensity (JCPDS 4-0850) of the (hkl) reflection.  $n$  is the number of reflections used in the calculation (in this case (111) for  $2\theta = 44.50$ , (200) for  $2\theta = 51.90$ , (220) for  $2\theta = 76.40$ , (311) for  $2\theta = 93.0$  and (222) for  $2\theta = 98.50$  were used). Atoms always incline to crystallization in crystal planes with lowest surface energy. According to Wang et al. [13] the relations between surface energies for nickel is:  $\gamma(111) < \gamma(100) < \gamma(110)$ . Hence, nickel atoms incline to crystallization in (111) crystal planes. The preferred texture of electrodeposits obtained at the current density of  $10 \text{ A/dm}^2$  is (200) texture, while at  $1 \text{ A/dm}^2$  a random texture was observed (Table II). This observation

may be associated with the fact that high current density leads to high growth rates, hence some of the nickel ions are

incapable of migrating to (111) plane, and would rest on (200) crystal plane.

TABLE II  
TEXTURE COEFFICIENTS OF (111), (200), (220), (311) AND (222) CRYSTAL PLANES

Electrodeposition parameters			TC (111)	TC (200)	TC (220)	TC (311)	TC (222)
$i$ (A/dm <sup>2</sup> )	$f$ (Hz)	$\gamma$ (%)					
1	10	50	1.57	1.19	0.11	1.64	0.47
10	10	50	1.32	2.94	0.11	0.3	0.45
4	1	50	1.73	0.77	0.42	1.3	0.77
4	100	50	2.12	1.42	0.1	0.92	0.49
4	10	25	1.34	2.77	0.26	0.34	0.29
4	10	75	1.42	0.7	0.41	2.46	0.19

In all the cases TC(111) would vary between 2.12 (nickel deposit produced at 100 Hz pulse frequency) and 1.32 (deposit obtained at applied current density of 10 A/dm<sup>2</sup>). TC(220) and TC (222) values always remained lower than 0.8 and 0.5 respectively. It seems that TC(200) is inversely connected to the TC(311). Increasing applied current density from 1 to 10 A/dm<sup>2</sup> resulted in 2.5 fold increase in TC(200) whereas the TC(311) at 10 A/dm<sup>2</sup> was one-fifth of TC(311) at 1 A/dm<sup>2</sup>. On the other hand, increasing duty cycle resulted in 4 fold decrease in TC(200) and considerably increased the (311) texture coefficient. Effect of pulse frequency on the coatings texture is not significant. However, TC(111) slightly increases with increasing pulse frequency

### C. Crystallite Size of the Deposits

Grain size measurements were performed using the Scherrer formula [14]:

$$D = \frac{k\lambda}{\beta \cos\theta} \quad (4)$$

where D is the size of crystallites,  $\lambda$  is x-ray wavelength (Cu K $\alpha$ : 0.15418 nm),  $\beta$  shows the peak width at half-maximum intensity in radiance, k is the shape factor (0.9) and  $\theta$  is bragg angle. Crystallite size values were calculated using (111) and (200) reflections. Table III presents the crystallite sizes of the electrodeposits obtained under different conditions.

The relationship between deposition overpotential  $\eta$  and current density/nucleation rate is given in:

$$\ln i = A - \frac{B}{(\eta)^2} \quad (5)$$

$$r = k_1 \exp\left(\frac{k_2}{\eta^2}\right) \quad (6)$$

The size of the crystallites increased with increasing current density. This seems unreasonable. From 5 and 6 we expected to see smaller crystallites at higher current densities. Ebrahimi et al. [15] have reported the same observation for nanocrystalline nickel coatings. They measured the overpotential and observed that it decreased with increasing

current density. This observation implies a complex current-electrode potential relationship. Cziraki et al. [16] attributed the increase in the crystallite size of the nickel electrodeposits obtained from a nickel Watts solution to a decline in the concentration of Ni cations at the cathode-electrolyte interface. The efficiency of Ni electrodeposition process decreases with increasing applied current, which means a relative decrease in the Ni<sup>2+</sup> ions concentration [7]. As the evolution of hydrogen is the main side reaction in nickel Watts bath, the decline in efficiency can be attributed to a higher rate of hydrogen evolution at the deposit-electrolyte interface. It has been established that hydrogen formation enhances planar growth in nickel [17]. Hence, it is reasonable that the change of the nickel growth interface by H<sub>2</sub> encourages the formation of larger crystallites.

The same behavior was observed for increasing duty cycle. Increasing duty cycle from 25% to 75% resulted in crystallite size increase from 32 to 44 nm ((111) reflection). Coarse crystallites at duty cycle of 75% may be attributed to the higher average current density. At high duty cycles on-time is much larger than the off-time and the pulse current is virtually a direct current (due to capacitance effect) [9]. This leads to a decrease in the Ni<sup>2+</sup> ions concentration at the cathode surface and consequently encourages hydrogen evolution. As it was mentioned earlier hydrogen formation at the deposit surface enhances planar growth in nickel and encourages the formation of larger crystallites. The effect of pulse frequency on crystallite size was insignificant and increasing pulse frequency slightly increased the crystallite size.

TABLE III  
CRYSTALLITE SIZE OF THE ELECTRODEPOSITS

Electrodeposition parameters			Crystallite size using (111) reflection (nm)	Crystallite size using (200) reflection (nm)
$i$ (A/dm <sup>2</sup> )	$f$ (Hz)	$\gamma$ (%)		
1	10	50	37	23
10	10	50	74	115
4	1	50	40	23
4	100	50	46	39
4	10	25	32	27
4	10	75	44	29

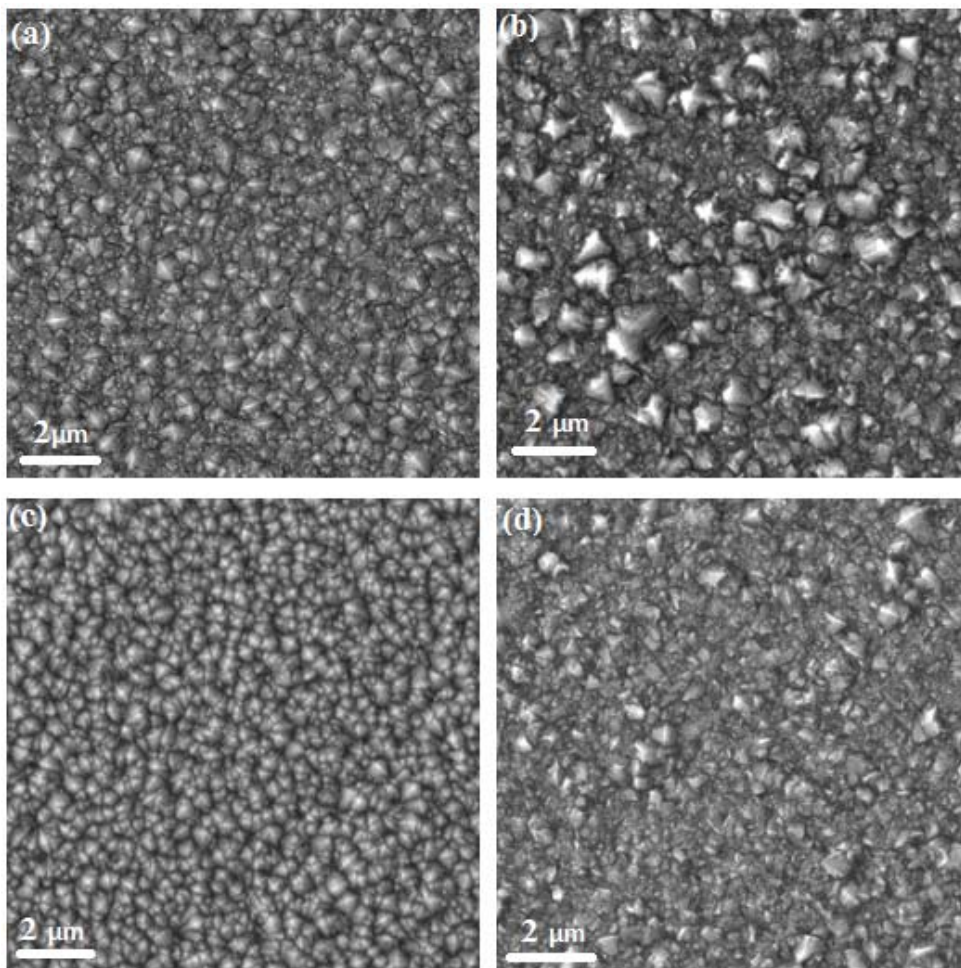


Fig. 2 SEM micrographs of Ni electrodeposits obtained at (a)  $i_p = 4 \text{ A/dm}^2$ ,  $\gamma = 50\%$ ,  $f = 10\text{Hz}$  (b)  $i_p = 10 \text{ A/dm}^2$ ,  $\gamma = 50\%$ ,  $f = 10\text{Hz}$  (c)  $i_p = 4 \text{ A/dm}^2$ ,  $\gamma = 75\%$ ,  $f = 10\text{Hz}$  (d)  $i_p = 4 \text{ A/dm}^2$ ,  $\gamma = 50\%$ ,  $f = 100\text{Hz}$

#### D. Morphological Studies

Fig. 2 shows that at high applied current densities, surface morphology of nickel electrodeposits is composed of several large pyramidal-shaped crystallites and fine grains at its surrounding. As the peak current density increases from 1 to  $10 \text{ A/dm}^2$  the size of the large crystals increases from about  $0.2$  to  $1 \mu\text{m}$ . The pyramidal growth of the nickel electrodeposits is attributed to field-oriented texture that is defined as preferential growth in the direction of electric field [18].

The decreased grain size at high applied currents may be attributed to:

1. Greater concentration polarization which results in the increase of overpotential and consequently decrease of the grain size (see
2. Increased hydrogen evolution at the cathode surface and consequently dramatic increase of pH at the deposit/solution interface. This enhances the adsorption or incorporation of  $\text{Ni(OH)}_2$ . The adsorption or deposition of  $\text{Ni(OH)}_2$  at the active growth sites of nickel deposit will

perturb the growth of nickel crystals, thus finer grained deposit will be formed.

The presence of some large pyramids at the current density of  $10 \text{ A/dm}^2$  seems unreasonable. According to [8] at high current densities the percentage of current for the evolution of hydrogen increases, leading to lower efficiency for nickel deposition, hence, nucleation rate of nickel decreases. These conditions encourages grain growth and results in the formation of coarse crystalline grains.

Effect of duty cycle on the morphology is presented in Fig. 2 (c). As the duty cycle raises from 10 to 75% the size of the grains decreases. This may be attributed to the higher average current density. In pulse electrodeposition the average current density can be calculated using:

$$i_a = \gamma \times i \quad (7)$$

Higher average current density leads to higher nucleation rates and consequently results in formation of finer grains.

TABLE IV  
MICROHARDNESS VALUES OF THE PURE NICKEL COATINGS OBTAINED UNDER DIFFERENT CONDITIONS

Electrodeposition parameters			Measurement	Measurement	Measurement	Average
i (A/dm <sup>2</sup> )	f (Hz)	γ(%)	1 (Hv)	2 (Hv)	3 (Hv)	(Hv)
1	10	50	196	179	184	186.3
10	10	50	140	150	150	146.7
4	1	50	142	150	146	146
4	100	50	145	156	151	150.6
4	10	25	201	182	196	193
4	10	75	122	120	125	122.3

### E. Microhardness Measurements

Table IV presents the microhardness values of the coatings. It has been reported that Nickel electrodeposits with the [100] preferred orientation show ductile behavior [19].

[211] growth mode is reported to commonly be associated to higher values of hardness [10]. Another important factor that affects microhardness of the materials is grain size. Hall-Petch equation correlates the yield stress and grain size of material:

$$\sigma_y = \sigma_0 + \frac{k}{\sqrt{d}} \quad (8)$$

This equation is based on the dislocation pile-up theory of metals. It can be seen in Table IV that the microhardness of the nickel decreased with increasing current density. As it was mentioned earlier nickel electrodeposit obtained at 10 A/dm<sup>2</sup> possesses larger grains. Also, at current density of 10 A/dm<sup>2</sup> TC(200) is 2.94 (Table II) which means that the preferred orientation of the coating is [100]. Hence, it is reasonable that the microhardness of the nickel electrodeposit obtained at 10 A/dm<sup>2</sup> is considerably lower than that of the electrodeposit obtained at 1 A/dm<sup>2</sup>. Increasing pulse frequency slightly increased the microhardness of the coatings. The grain size of the coating obtained at 100 Hz is larger which encourages a ductile behavior. However, a higher TC(111) at 100 Hz improves the hardness of the coating. Finally, the microhardness of the nickel deposits decreased with increasing duty cycle. Although, at γ=75% TC(200) is low (0.7) but a high crystallite size resulted in decline of the microhardness.

### REFERENCES

- [1] H. Omidvar, M. Sajjadnejad, G. Stremsoerfer, Y. Meas, and A. Mozafari, "Manufacturing Ternary Alloy NiBP-PTFE Composite Coatings by Dynamic Chemical Plating Process", *Mater. Manuf. Process.*, 2015 (just accepted).
- [2] M. Sajjadnejad, M. Ghorbani, and A. Afshar, "Microstructure-corrosion resistance relationship of direct and pulse current electrodeposited Zn-TiO<sub>2</sub> nanocomposite coatings", *Ceram. Int.*, Vol. 41, No. 1, pp. 217-224, 2015.
- [3] A. El-Sherik and U. Erb, "Synthesis of bulk nanocrystalline nickel by pulsed electrodeposition", *J. Mater. Sci.*, Vol. 30, No. 22, pp. 5743-5749, 1995.
- [4] C.A. Huang, C.Y. Chen, C.C. Hsu, and C.S. Lin, "Characterization of Cr-Ni multilayers electroplated from a chromium (III)-nickel (II) bath using pulse current", *Scr. mater.*, Vol. 57, No. 1, pp. 61-64, 2007.
- [5] Y. Li, H. Jiang, W. Huang, and H. Tian, "Effects of peak current density on the mechanical properties of nanocrystalline Ni-Co alloys produced by pulse electrodeposition", *Appl. Surf. Sci.*, Vol. 254, No. 21, pp. 6865-6869, 2008.
- [6] M. Sajjadnejad, A. Mozafari, H. Omidvar, and M. Javanbakht, "Preparation and corrosion resistance of pulse electrodeposited Zn and Zn-SiC nanocomposite coatings", *Appl. Surf. Sci.*, Vol. 300, No. pp. 1-7, 2014.
- [7] M. Schlesinger and M. Paunovic, *Modern electroplating*, New York, John Wiley & Sons, 2011, Ch.3.
- [8] Y. Xuetao, W. Yu, S. Dongbai, and Y. Hongying, "Influence of pulse parameters on the microstructure and microhardness of nickel electrodeposits", *Surf. Coat. Technol.*, Vol. 202, No. 9, pp. 1895-1903, 2008.
- [9] M. Chandrasekar and M. Pushpavanam, "Pulse and pulse reverse plating—Conceptual, advantages and applications", *Electrochim. Acta*, Vol. 53, No. 8, pp. 3313-3322, 2008.
- [10] N.A. Badarulzaman, A.A. Mohamad, S. Puwadaria, and Z.A. Ahmad, "The evaluation of nickel deposit obtained via Watts electrolyte at ambient temperature", *J.coat. technol. research*, Vol. 7, No. 6, pp. 815-820, 2010.
- [11] C. Kollia, N. Spyrellis, J. Amblard, M. Froment, and G. Maurin, "Nickel plating by pulse electrolysis: textural and microstructural modifications due to adsorption/desorption phenomena", *J. appl. electrochem.*, Vol. 20, No. 6, pp. 1025-1032, 1990.
- [12] L. Chen, L. Wang, Z. Zeng, and T. Xu, "Influence of pulse frequency on the microstructure and wear resistance of electrodeposited Ni-Al<sub>2</sub>O<sub>3</sub> composite coatings", *Surf. Coat. Technol.*, Vol. 201, No. 3, pp. 599-605, 2006.
- [13] S. Wang, E. Tian, and C. Lung, "Surface energy of arbitrary crystal plane of bcc and fcc metals", *J.Physic. Chem. Solid.*, Vol. 61, No. 8, pp. 1295-1300, 2000.
- [14] H. Sohrabi, S. Tabaian, H. Omidvar, M. Sajjadnejad, and A. Mozafari, "Synthesis of Nanostructured TiO<sub>2</sub> Coatings by Sol-Gel Method: Structural and Morphological Studies", *Synth. React. Inorg. M.*, 2015 (just accepted).
- [15] F. Ebrahimi and Z. Ahmed, "The effect of current density on properties of electrodeposited nanocrystalline nickel", *J. appl. electrochem.*, Vol. 33, No. 8, pp. 733-739, 2003.
- [16] A. Cziraki, B. Fogarassy, I. Geröcs, E. Tóth-Kádár, and I. Bakonyi, "Microstructure and growth of electrodeposited nanocrystalline nickel foils", *J. mater. sci.*, Vol. 29, No. 18, pp. 4771-4777, 1994.
- [17] K. Haug and T. Jenkins, "Effects of hydrogen on the three-dimensional epitaxial growth of Ni (100),(110), and (111) ", *The J.Physic. Chem. B*, Vol. 104, No. 43, pp. 10017-10023, 2000.
- [18] S.A. Calbeto, "Nickel matrix micro/nano SiC composite electrodeposition". 2011, Polytechnic University of Catalonia. p. 53.
- [19] I. Matsui, Y. Takigawa, T. Uesugi, and K. Higashi, "Enhanced tensile ductility in bulk nanocrystalline nickel electrodeposited by sulfamate bath", *Mater. Letter.*, Vol. 65, No. 15, pp. 2351-2353, 2011.